EUROPEAN ORGANIZATION FOR NUCLEAR RESEARCH

Proposal to the ISOLDE and Neutron Time-of-Flight Committee

(Following HIE-ISOLDE Letter of Intent I-102)

Precision tests of shape coexistence in the light Krypton nuclei

3rd October 2012

D.G. Jenkins[1], C.J. Barton[1], P.J. Davies[1], B.P.Kay[1], R. Wadsworth[1], W. Catford[2], S. Freeman[3], M. Labiche[4], A.H. Wuosmaa[5], F. Flavigny[6], R. Orlandi[6], R. Raabe[6],P. Butler[7], L. Gaffney[7], D.T. Joss[7], G. O'Neill[7], R.D. Page[7], D. Muecher[8], R. Gerhauser[8], S. Klupp[8], K. Nowak[8] on behalf of the solenoidal spectrometer collaboration

[1] Department of Physics, University of York, York, YO10 5DD, UK
[2] Department of Physics, University of Surrey, Guildford GU2 7XH, UK
[3] School of Physics and Astronomy, University of Manchester, Manchester M13 9PL, UK
[4] STFC Daresbury Laboratory, Warrington WA4 4AD, UK
[5] Department of Physics, Western Michigan University, Kalamazoo, MI-49008
[6] KU Leuven, B-3001 Heverlee, Belgium
[7] Department of Physics, University of Liverpool, Liverpool L69 7ZE, UK
[8] Physik Department, TU Muenchen, D-87548 Garching, Germany

Spokesperson(s): David Jenkins (david.jenkins@york.ac.uk), Wilton Catford (w.catford@surrey.ac.uk)
Local contact: Magda Kowalska (Magdalena.Kowalska@cern.ch)

CERN-INTC-2012-048 / INTC-P-349
02/10/2012

Abstract

We propose to obtain a microscopic understanding of shape coexistence in the region close to ^{72}Kr by studying the ^{74}Kr(d,p) and ^{76}Kr(d,p) reactions in inverse kinematics at 5.5 MeV/u. The outgoing protons will be analysed using a solenoidal spectrometer. The intention is to achieve a microscopic understanding of the shape coexistence in the proton-rich nuclei around mass 70. This will pose a strong test of state-of-the-art models of the shape coexistence phenomenon.

Requested shifts: 33 shifts, (split into 2 runs over 1 or 2 years)
Beamline: 2nd beamline

Introduction: A remarkable feature of the atomic nucleus is its ability, under certain circumstances, to take on different mean-field shapes for a small cost in energy compared to the total binding energy of the nucleus. A spectacular example of this phenomenon is in the light lead nuclei, for example, ^{186}Pb where two excited 0^+ states associated with a prolate and oblate deformed minimum coexist with a spherical ground state within an excitation energy range of less than 1 MeV. A second notable region of shape coexistence is the region close to the N=Z line for A~70. Here there is a rapidly changing nuclear shape evolving from the spherical nucleus, ^{56}Ni with doubly-closed shell, through nuclei like ^{64}Ge which are suggested to be triaxial, to ^{68}Se [Fis00] and ^{72}Kr [Fis01,Fis03] which are believed to exhibit a close competition between oblate and prolate minima [Pet02,Lal99,Naz85]. The shape coexistence in this region is said to be driven by increasing occupation of the $g_{9/2}$ orbital.
In the past, shape coexistence has largely been inferred from in-beam studies, where the layout of levels and the presence of multiple excited bands has been attributed to different mean-field configurations. In certain special cases, for example, ^{72}Kr, electron spectroscopy has been used where the lowest excited state has, highly unusually, spin/parity of 0^+ [Bou03]. Laser spectroscopy has also been used to map out changes in nuclear radius and deformation but this is only applicable to the ground state or long-lived metastable states. A breakthrough in the study of shape coexistence has come about through the availability of intense re-accelerated radioactive beams. Such beams can be employed in Coulomb excitation studies. Coulomb excitation is a very useful technique for examining nuclear collectivity through extraction of transition matrix elements. Such matrix elements can also be extracted from lifetime measurements but the techniques are complementary as states are excited from the ground state up in Coulomb excitation, often leading to a very different level population from in-beam lifetime studies. The principal advantage of Coulomb excitation, however, is the possibility to extract diagonal matrix elements through the second-order process of reorientation. Such matrix elements allow the sign of the spectroscopic quadrupole moment to be extracted and, hence, the sign of the associated nuclear deformation. An excellent example of this technique is the Coulomb excitation of ^{74}Kr and ^{76}Kr [Cle07], where a large number of matrix elements were extracted (see figure 1). The data were such as to allow discrimination between competing mean-field descriptions [Cle07].

The focus of the present proposal is to complement the very detailed Coulomb excitation study with a more microscopic understanding of the shape coexistence phenomenon in this region. This will be achieved by carrying out a study of the ^{74}Kr(d,p) and ^{76}Kr(d,p) reaction in inverse kinematics. Existing potential energy surface calculations tally with the findings from Coulomb excitation of substantial deformation in this region and suggest that the lowest prolate deformed orbits are $3/2^+[431]$, $3/2^-[312]$ and $3/2^-[301]$ Nilsson configurations which are dominated by components of the $g_{9/2}$, $f_{5/2}$ and $p_{3/2}$ spherical shell model states respectively. Identification of the $g_{9/2}$ strength in particular should reveal a great deal about the nature of the deformation encountered. The intruder nature of this orbit means that the deformed orbits stemming from it maintain their single-particle purity. Transfer on deformed nuclei is more challenging but still very valuable as "fingerprints" of deformation can be obtained [Elb69]. Detailed spectroscopic information on excited states in ^{75}Kr and ^{77}Kr is available from in-beam studies [Tab99] as well as beta decay [Mol82]. In the case of ^{77}Kr, there is also information deriving from a ^{78}Kr(p,d) study [Ogi77]. In general, the excited states up to 0.5 MeV and beyond are well determined.

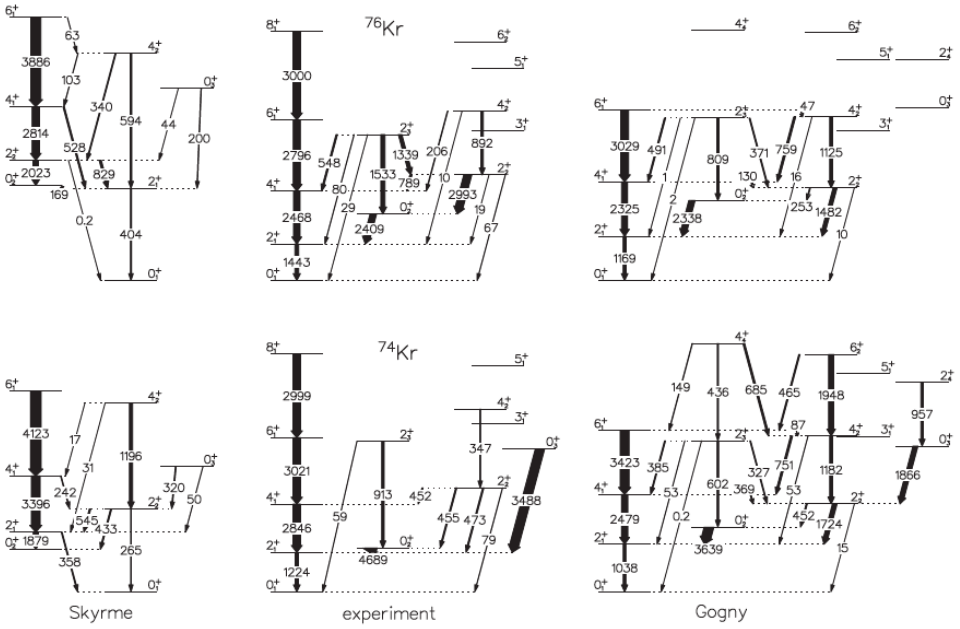

Figure 1: Comparison of transition strengths extracted from Coulomb excitation for ^{74}Kr and ^{76}Kr compared with different mean field models (taken from figure 16 of [Cle07]). The numbers on the transitions refer to the transition strength.

In the past, transfer reactions have been carried out on the stable light Krypton isotopes including ^{78,80,82}(d,p) by Chao et al. [Cha75] (see figure 2). Typical cross-sections for (d,p) on the heavier Krypton isotopes were found to be of the order of mb/sr. This study allowed the different excited levels to be mapped out and strength for different orbitals to be extracted (see figure 3).

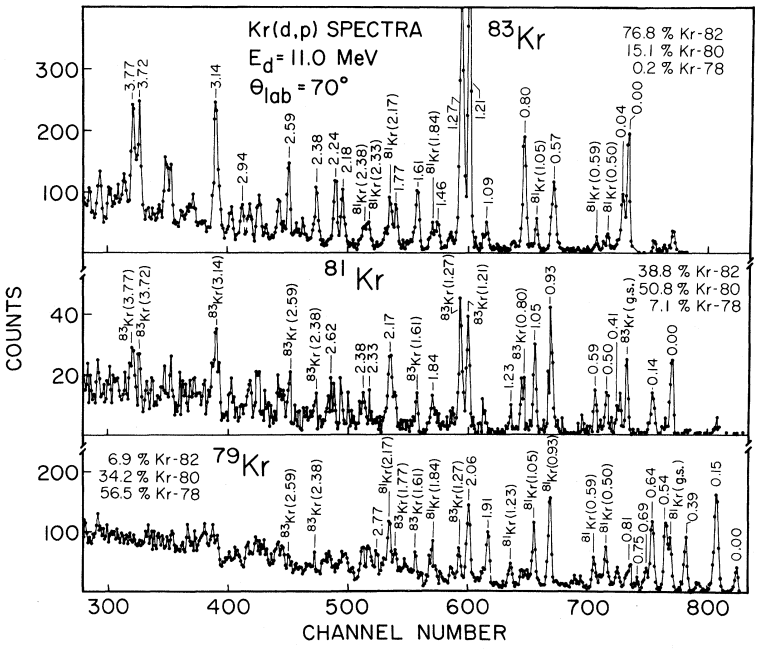

Figure 2: Proton spectra for (d,p) studies on the light stable Krypton isotopes from [Cha75]

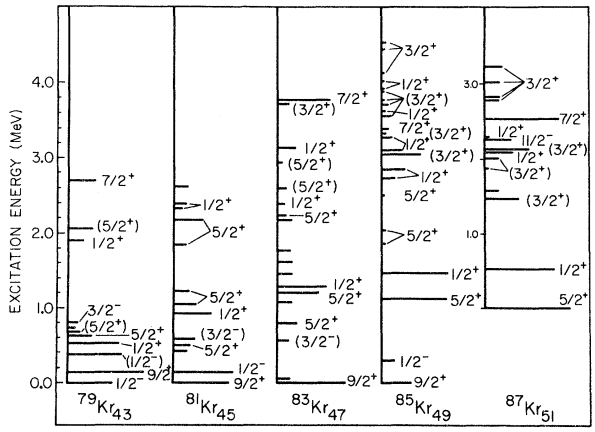

Figure 3: Energy level diagrams from Kr(d,p) studies. The length of the lines is proportional to the spectroscopic factors (taken from [Cha75])

Experiment: The experiment will use a solenoidal spectrometer for momentum analysis of the outgoing protons from the reaction, similar to that in use at Argonne National Laboratory [Lig10, Wuo07]. In such a spectrometer illustrated in figure 4, the radioactive beam is incident on a deuterated plastic target at the centre of a large solenoidal magnet of the type used for MRI scanners. The protons from the (d,p) reaction follow helical orbits in the magnetic field and are recorded in a compact, linear silicon array covering backward angles in the lab frame. This design of spectrometer has three significant advantages over conventional charged-particle spectroscopy using silicon detectors, beyond the solenoid representing a much simpler and less complex detector system. Firstly, better proton energy resolution where it is not limited by target energy loss effects. This arises due to the linear function between centre-of-mass energy and the measured position and lab energy measured at the axis of the solenoid. Essentially, the lab ion energy resolution is identical to the CM energy resolution. Secondly, the linear nature of this relationship also means that the dispersion different excited states in the ion-energy and Q-value spectra are the same. In the conventional approach using Si at fixed angles, the non-linear relationship between proton energy and angle can mean that when moving from an ion energy spectrum to excitation energy, peaks become compressed by factors of up to three, degrading the effective Q-value resolution. Even for experiments where target energy-loss effects are important in the ion-energy resolution, the resulting Q-value spectrum with a solenoid still benefits from this lack of compression. As an example, a recent d(^{86}Kr,p) measurement achieved an excitation energy resolution of ~70 keV. Some conventional approaches use γ-ray measurements to recover the excitation energy resolution. This necessarily introduces an additional efficiency factor of up to 10% due to the coincidence requirement but this can be mitigated to some extent by using a thicker target. A solenoidal system allows good resolution, sufficient for many purposes, from the measurement of outgoing ions alone and thus avoids the efficiency hit in yield for many experiments.

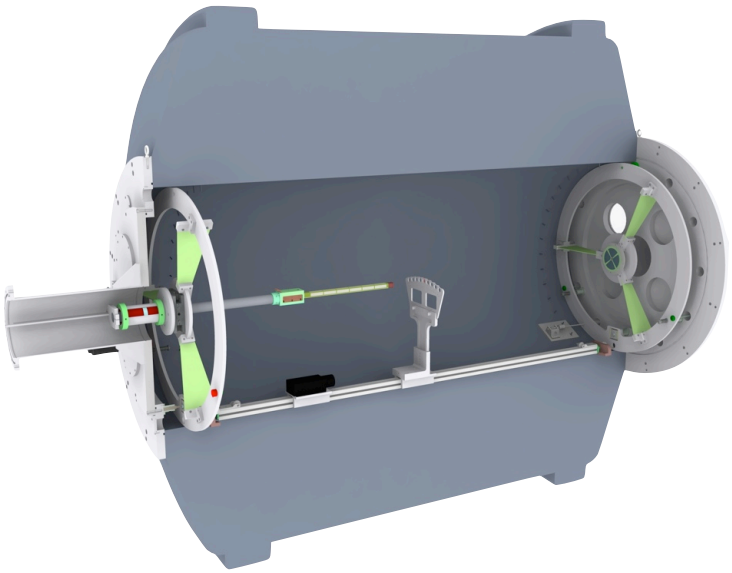

Figure 4: Schematic of a solenoidal spectrometer. The beam enters from the left hand side and is incident on a target at the centre. Protons are detected along the solenoid axis.

In the present experiment, the silicon array will be positioned at backward angles in the lab. The total length of the array is 70-cm and comprises 10 detectors. Each detector has an active area of 50-mm long and 9-mm wide, and is 700-μg thick. Position sensitivity is achieved by resistive charge division. In order to extract absolute cross sections, the product of the beam intensity and the areal density of deuterons in the target will be measured throughout the experiment. An annular Si surface-barrier detector positioned downstream from the target such that elastically scattered deuterons are intercepted and the luminosity deduced from the yield. Figure 5 presents a simulation of the kinematics and expected angular distributions for the ^{76}Kr(d,p) reaction at a beam energy of 5.5 MeV/u. The expected Q-value resolution is 70 keV for a 100 ug/cm^2 CD_2 target. While the simulated spectrum is complicated, we anticipate that the very good energy resolution allied to the pre-existing knowledge of the location of excited states originating from earlier in-beam or beta-decay measurements with germanium detector arrays will permit us to fit the peak areas corresponding to different states, at least for states up to 1 MeV. At a certain point, we are likely to encounter levels not known from beta decay or in beam and this will limit our sensitivity.

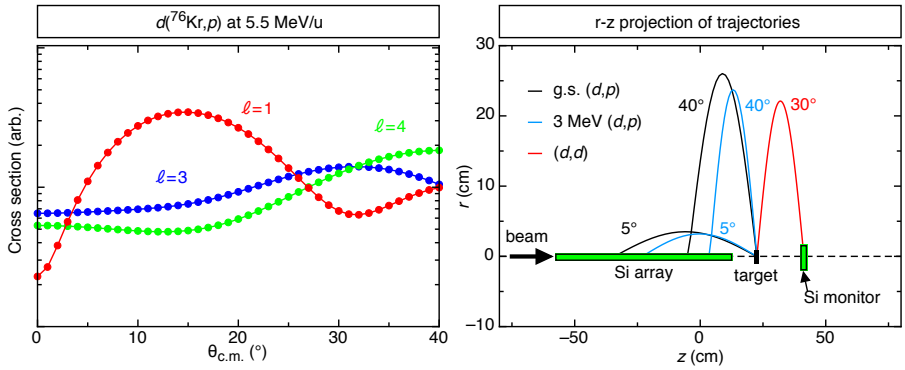

Figure 5: The left-hand panel shows the angular distribution and cross-section dependence expected for the 76Kr(d,p) reaction as a function of c.m. angle. The right-hand panel shows the trajectories of different light ions for (d,p) and (d,d') reactions as a function of c.m. angle.

We can estimate rates on the basis of experience with radioactive beam transfer experiments. The limit for thin target measurements with a one-week study is around 10^4 s^{-1}. We assume a 3% transmission efficiency from the ISOLDE target to the delivered radioactive beam on target. Taking the best measured yield for ^{76}Kr from a Nb target of 1.2 X 10^8 s^{-1} implies a beam on target of around 3.6 X 10^6 s^{-1}. For ^{74}Kr the best yield from a Nb target is 6 X 10^6 s^{-1} implying 1.8 X 10^4 s^{-1}. This would be on the limit for a one-week experiment. A key factor is that the beam will be 100% pure through the use of a cooled transfer line and we will not have the limiting effects of target contamination encountered in the early (d,p) studies of light Kr isotopes using enriched gas targets.

Summary of requested shifts:

We propose to conduct this experiment in two phases. In phase 1, we will setup with a stable beam like ^{78}Kr or ^{80}Kr and perform a (d,p) study to calibrate the system and evaluate the performance with respect to the earlier work in normal kinematics. We request 12 shifts for the ^{76}Kr(d,p) study to obtain good statistics for angular distributions and to obtain spectroscopic factors. In phase 2, we request 21 shifts to carry out the more challenging ^{74}Kr(d,p) study.

References:

[Cle07] E. Clement et al., Phys. Rev. C 75, 054313 (2007).

[Lig10] J.C. Lighthall et al., NIM A 622, 97 (2010).

[Wuo07] A.H. Wuosmaa et al., NIM A 580, 1290 (2007).

[Cha75] J. Chao et al., Phys. Rev. C 11, 1237 (1975).

[Elb69] B. Elbeck and P.O. Tjom, Adv. in Nucl. Phys. 3, 259 (1969).

[Fis00] S.M. Fischer et al., Phys. Rev. Lett. 84, 4064 (2000).

[Pet02] A. Petrovici, K. W. Schmidt and A. Faessler, Nucl. Phys. A 710, 246 (2001).

[Lal99] Lalazissis et al., Nucl. Data Tables 71, 1 (1999).

[Naz85] W. Nazarewicz et al., Nucl. Phys. A 435, 397 (1985).

[Ogi77] K. Ogino et al., Univ. Tokyo, Ann. Rept., p.26 (1977)

[Tab99] S.L. Tabor and G.Z. Solomon, J. Phys. G 25, 763 (1999).

[Mol82] D.M. Moltz et al., Phys. Lett. B113, 16 (1982).

[Bou03] E. Bouchez et al., Phys. Rev. Lett. 90, 082502 (2003).

[Fis01] S.M. Fischer et al., Phys. Rev. Lett. 87, 132501 (2001).

[Fis03] S.M. Fischer et al., Phys. Rev. C 67, 064318 (2003).

Appendix

DESCRIPTION OF THE PROPOSED EXPERIMENT

The experimental setup comprises: *Helical-orbit spectrometer*

Part of the Choose an item.	Availability	Design and manufacturing
	☐ Existing	☐ To be used without any modification
Helical-orbit spectrometer on second beamline	☐ Existing	☐ To be used without any modification ☐ To be modified
	☒ New	☐ Standard equipment supplied by a manufacturer ☒ CERN/collaboration responsible for the design and/or manufacturing
	☐ Existing	☐ To be used without any modification ☐ To be modified
	☐ New	☐ Standard equipment supplied by a manufacturer ☐ CERN/collaboration responsible for the design and/or manufacturing

HAZARDS GENERATED BY THE EXPERIMENT

Additional hazards:

Hazards	*76Kr(d,p)*	*74Kr(d,p)*	*[Part 3 of the experiment/equipment]*
Thermodynamic and fluidic			
Pressure			
Vacuum			
Temperature			
Heat transfer			
Thermal properties of materials			
Cryogenic fluid	LHe, 1650 [l] LN_2, 200 [l]		
Electrical and electromagnetic			
Electricity	[voltage] [V], [current][A]		
Static electricity			
Magnetic field	3 [T]		
Batteries	☐		
Capacitors	☐		
Ionizing radiation			
Target material	Nb	Nb	
Beam particle type (e, p, ions, etc)	76Kr	74Kr	
Beam intensity	4 X 10^6 s^{-1}	2 X 10^4 s^{-1}	
Beam energy	5.5 MeV/u	5.5 MeV/u	
Cooling liquids	[liquid]		
Gases	[gas]		
Calibration sources:	☒		
• Open source	☐		

• Sealed source	☒ [ISO standard]		
• Isotope			
• Activity			
Use of activated material:			
• Description	☐		
• Dose rate on contact and in 10 cm distance	[dose][mSV]		
• Isotope			
• Activity			
Non-ionizing radiation			
Laser			
UV light			
Microwaves (300MHz-30 GHz)			
Radiofrequency (1-300MHz)			
Chemical			
Toxic	[chemical agent], [quantity]		
Harmful	[chemical agent], [quantity]		
CMR (carcinogens, mutagens and substances toxic to reproduction)	[chemical agent], [quantity]		
Corrosive	[chemical agent], [quantity]		
Irritant	[chemical agent], [quantity]		
Flammable	[chemical agent], [quantity]		
Oxidizing	[chemical agent], [quantity]		
Explosiveness	[chemical agent], [quantity]		
Asphyxiant	[chemical agent], [quantity]		
Dangerous for the environment	[chemical agent], [quantity]		
Mechanical			
Physical impact or mechanical energy (moving parts)	[location]		
Mechanical properties (Sharp, rough, slippery)	[location]		
Vibration	[location]		
Vehicles and Means of Transport	[location]		
Noise			
Frequency	[frequency],[Hz]		
Intensity			
Physical			
Confined spaces	[location]		
High workplaces	[location]		
Access to high workplaces	[location]		
Obstructions in passageways	[location]		
Manual handling	[location]		
Poor ergonomics	[location]		

0.1 Hazard identification

3.2 Average electrical power requirements (excluding fixed ISOLDE-installation mentioned above): *(make a rough estimate of the total power consumption of the additional equipment used in the experiment)*

… kW